Determination of the synergism/antagonism parameters during co-gasification of potassium rich biomass with non-biomass feedstock

Roxin Fernandes[1], *Josephine M. Hill*[2] *and Jan Kopyscinski*[1]

[1]Department of Chemical Engineering, McGill University, 3610 University Street, Montreal, Canada

[2]Department of Chemical & Petroleum Engineering, University of Calgary, 2500 University Drive NW, Calgary, Canada

**Email:* jan.kopyscinski@mcgill.ca, *Tel.:* +1 514 398 4276

Abstract

This study focuses on quantifying the synergistic/antagonistic behaviour occurring during the co-gasification of non-biomass feedstock (ash-free coal, fluid coke) with potassium-rich switchgrass. The results showed that the gasification rate of switchgrass in the mixture decreased as a certain amount of its potassium was transferred to the non-biomass feed leading to a multifold increase in non-biomass gasification rate. The aim of this study was to quantify this behaviour through kinetic modeling. It was assumed that each constituent in the mixture follows the random pore model with their corresponding kinetic parameters. Furthermore, synergism/antagonism parameters were included, which were either a constant or a function of the switchgrass conversion (linear, square root) representing the effect of inter-particle potassium mobility. The acceleration of the gasification rate of the non-biomass feedstock followed a linear function of the switchgrass conversion. The inhibition of the switchgrass conversion did not show a clear trend as it depends on the non-biomass feedstock and temperature. The presence of potassium in switchgrass which acts as a catalyst is clearly observed from the modeling, where the gasification rates for the fluid coke or ash-free coal in the mixture significantly increased for all temperatures studied. Modeling

of the gasification reactions with the estimated best-fit synergism/ antagonism models showed a very good agreement with the observed values. The obtained results of this study can be useful in designing co-gasification systems and estimating the best ratio of biomass to non-biomass feeds.

1 Introduction

Co-gasification has been studied for a variety of biomass/non-biomass combinations (e.g., wood/coal, switchgrass/coal, switchgrass/petroleum coke)[1–6]. Gasification of coal or petroleum coke alone is a slow process, but the addition of biomass can reduce the gasification time[5,7,8]. In that sense biomass is not only a fuel but also enhances gasification of the non-biomass feed. General benefits of co-gasification are reduced fossil fuel related greenhouse gas emissions, lower tar formation, higher overall efficiency and increased char reactivity. The latter, is mostly explained due to inherently present alkali and/or alkali earth metals (e.g., potassium, sodium, calcium) in the biomass that act as a catalyst and enhance the gasification rate[1,5,6]. For example, potassium is highly mobile under gasification conditions and can transfer (interparticle) from the biomass to the non-biomass feed as demonstrated with our previous work[5]. The addition of synthetic catalysts is also known to significantly enhance gasification, but this is associated with high cost, catalyst preparation and recovery complications[9]. The use of biomass feedstock might be more economical as it acts as a natural and inexpensive catalyst for the conversion of solid fossil fuels.

Many studies have investigated the interaction between biomass and non-biomass feeds during co-gasification. Depending on the type of fuel, ratio of biomass to non-biomass, temperature and type of experiments (e.g., gasification of char mixture, combined pyrolysis and gasification) synergistic effects, inhibition effects and no interaction have been observed[3,5,6,9,10]. For example, co-gasifying switchgrass char (high potassium content) with coal char (high ash content) showed an inhibition effect during CO_2 gasification (i.e., gasification rate of the switchgrass-coal mixture was equal to or slower than the gasification rate of coal itself)[5]. This behavior was attributed to sequestration of the mobile alkali elements (originated from the switchgrass) by the reaction with aluminosilicate minerals in coal to form inactive alkali aluminosilicates, such as $KAlSi_3O_8$ and $KAlSiO_4$. The potassium was not accessible to accelerate the gasification reaction. Catalytic activity was evident when excess alkali ($K/Al > 1$) was present in the feed mixture to satisfy the stoichiometric requirements of these deactivation reactions[5]. Similar behavior was observed for the gasification of corn stalk and with various types of coal[6]. Fossil fuels with low ash contents are the most suitable candidates to be co-gasified with a potassium rich biomass to benefit from the synergistic effect.

In the search for alternative means for energy production and sustainable energy development, studies on understanding the synergistic/antagonistic effects of biomass/fossil fuel co-gasification have been increasing. However, published literature focusing on quantifying these effects within a kinetic analysis are scarce. The present work deals with this issue and builds on our previous work of co-gasifying potassium-rich switchgrass with coal and fluid coke using CO_2 as gasifying agent[5]. In detail, the main goal of this study is to quantify and to better understand the observed synergism and antagonism behavior during the co-gasification of potassium-rich switchgrass with ash-free coal and fluid coke at different temperatures. A kinetic study including data collection (gasification experiments), model development, kinetic parameter estimation and model discrimination has been conducted.

2 Experimental

2.1 Biomass and Non-biomass Samples

Potassium-rich switchgrass (SG) (from Manitoba, Canada) was the biomass sample, while fluid coke (FC) (Syncrude, Alberta, Canada) and ash-free sub-bituminous coal (AFC) (Genesee, Alberta, Canada) were the non-biomass samples used in this study. Table 1 summarizes the proximate, ultimate and ash-analyses of the three parent feedstocks; these data have been published in previous studies[5,11]. The AFC had a very high amount of volatile matter and a low fixed carbon content of 69.5 and 30.5 wt% dry basis, respectively, whereas, fluid coke had a low ash, low volatile matter and high fixed carbon contents of 2.0, 6.9 and 91.1 wt% dry basis, respectively. Switchgrass has the highest potassium content as well as significant amounts of calcium and magnesium, which likely promote the catalytic co-gasification of the non-biomass feedstock. As both non-biomass samples (AFC and FC) had less than 2 wt% ash they will not contribute significantly towards catalyst deactivation as described above.

2.2 Char and Ash-free Coal Preparation

Ash-free coal was produced by solvent extraction as described in [11,12]. Briefly, the dry pulverised coal is mixed with an industrial solvent for extraction. The coal-solvent slurry is then heated in an inert atmosphere followed by filtration. In order to precipitate the filtrate, hexane is added, then filtered and dried in vacuum to obtain the ash-free coal sample.

For the switchgrass and fluid coke char preparation, approximately 5-10 g of the parent sample was heated to the desired temperature (e.g., 750-950°C) at atmospheric pressure in a quartz glass reactor (25 mm ID). A high heating rate was used: 25°C min^{-1} with 200 ml_N min^{-1} of N_2 (Praxair, 99.999%). All samples were ball milled and sieved to particle sizes of less than 90 µm. Ash-free coal samples were not charred prior to the gasification experiments. More details about sample preparation can be found in our previous studies[5,11,13].

2.3 CO_2 Gasification Experiments

The CO_2 gasification experiments were carried out in a thermogravimetric analyzer (Thermo Scientific, TGA Thermax 500) as described in [5,14]. Briefly, 10 mg of sample (i.e., single char or a targeted 50:50 by weight mixture for co-gasification) was placed in the reactor and heated at a rate of 15°C min^{-1} to the desired temperature (i.e., 750-950°C) under N_2 (400 ml_N min^{-1}, Praxair, 99.999%) atmosphere while the mass change was monitored. After a further holding time in N_2 at the isothermal temperature, the gas was switched to CO_2 (400 ml_N min^{-1}, Praxair, 99.99%). At this point the gasification time was defined as $t = 0$.

All gasification experiments were conducted isothermally at ambient pressure and at 850°C and 950°C for switchgrass/fluid coke (SG/FC) mixtures, while switchgrass/ash-free coal (SG/AFC) experiments were conducted at 750°C, 850°C and 950°C. Gasification experiments with FC at 750°C showed low reactivity and hence were not studied[5]. Prior to calculating the char conversion and gasification rates, the measured data (i.e., mass as a function of time) were smoothed in order to reduce the quantity of the data. During the experiments, the TGA software recorded the mass every two seconds, which resulted in up to 150000 data points over a run. The locally weighted scatterplot smoothing (LOWESS)[15] function was applied to smooth and reduce the number of data points to approximately 500-1000 per experiment. The char conversion is defined as,

$$X = \frac{m_o - m_t}{m_o - m_{end}} \tag{1}$$

where m_o is the initial mass at gasification time $t = 0$, m_t is the mass at time t and m_{end} is the mass after complete conversion (end of the experiment). Due to the small sample weight used and the solid dry mixing process (i.e., non-homogeneous distribution), the results (conversion vs. time) of repeated experiments varied within 10%. The variation between the same repeated experiments, however, was very small compared to the change in conversion for different experimental conditions (i.e., temperature).

3 Experimental Results

Figure 1 illustrates the CO_2 gasification behavior of SG, AFC and FC as single feeds as well as mixed feeds, at 850°C and 950°C. In addition to the experimental observations (dotted lines), the theoretical char conversion (solid lines) of the mixture is calculated based on the weighted average of the single feed conversions assuming no interaction between the constituents (eq. 2):

$$X_{non-interacting\ mix} = \beta \cdot X_{FF} + (1 - \beta) \cdot X_{SG} \tag{2}$$

where β is the mass fraction of the non-biomass char in the mixture (i.e., $\beta = 0.5$ in this study), and X_{FF} and X_{SG} are the conversions of the fossil fuel and SG, respectively.

As a reminder, the switchgrass and fluid coke were converted to char before gasification, while ash-free coal was used directly. SG refers to switchgrass char, FC refers to fluid coke char and AFC refers to ash-free coal throughout the remainder of the manuscript.

Although the gasification behavior of SG/FC has previously been published[5], it has been included again here (Figure 1) as these experimental data were used for the kinetic modeling and for comparison to the SG/AFC mixtures. SG is converted much faster than FC or AFC, requiring only 1.5 h for complete conversion at 850°C and ~18 min at 950°C. This fast conversion of SG is attributed to its high potassium content as well as high micropore surface area[5].

Individually, FC and AFC had similar slow gasification rates (Figure 1). At 850°C and 950°C complete conversion required ~ 50 h and 15 h, respectively, for FC, and ~ 70 h and 17 h, respectively, for AFC. The slow conversion rates reflect the low mineral (and hence catalyst) contents of these feeds. Adding switchgrass char accelerated significantly the conversion rates of both fluid coke (SG/FC) and ash-free coal (SG/AFC). The mixture of SG/FC was completely converted after 10 h at 850°C and 8 h at 950°C, while the mixture of SG/AFC was completely converted after 10 h at 850°C and 3 h at 950°C. At the higher temperature, the synergistic effect for AFC was larger, and, thus the addition of SG was somewhat different for AFC than on FC.

Comparison of the observed gasification behavior for the SG/FC and SG/AFC mixtures with the calculated non-interacting behavior (solid line, Figure 1) indicates both antagonism and synergism effects. The elementary steps of the catalyzed gasification process provide some understanding towards these effects. During the gasification, the potassium in SG acts as a catalyst and undergoes an oxygen transfer cycle in which the catalyst is being reduced and oxidized[16,17]. The precise form of the potassium catalyst in sample is unknown; however, the catalyst takes oxygen from the reaction gas (step 1) and transfers it to the surface where the oxygen reacts with the carbon to form carbon monoxide (step 2) as illustrated in Figure 2. The third step is site regeneration, which requires a certain potassium mobility (intra- and interparticle) - here designated non-specifically as $K\sim$. Note, K-C, $K\sim$ and $CO^{-}K^{+}$ represent generalized sites (i.e., reduced, reduced and oxidized, respectively) with the required potassium-carbon contact, but an unknown stoichiometry. Once a SG based carbon is converted, the potassium can either move to the next carbon within SG or move to the non-biomass (FC, AFC) sample, see Figure 2 step (3) or (3'), respectively. The observed gasification behavior of the mixture indicates the latter, as the conversion curve (dotted line in Figure 1) is below the non-interacting (solid) line until 50% conversion is reached (Figure 1). Thereafter the observed (dotted) line is above non-interacting line indicating a synergistic effect – that is, a significant increase in the gasification rate of the non-biomass sample. Assuming potassium would first accelerate the gasification of SG before accelerating the gasification of the non-biomass sample, then the observed conversion curve of the mixtures (SG/FC and SG/AFC) would follow the non-interacting curve until switchgrass is completely converted (i.e., 50% conversion of 50/50 mixture) and thereafter would be above the non-interacting line, which is not the case.

4 Parameter Estimation and Model Discrimination

4.1 Single Feedstock

The measured mass change in a given time interval was differential compared to the total mass (i.e., 0.001-0.05 mg min^{-1} vs. 10 mg) and CO_2 was fed in excess (400 ml_N min^{-1}). Thus, the CO_2 partial pressure did not change significantly. In addition, the produced CO was on the order of a in the order of 10-1000 ppmV (depending on sample and temperature, not shown). For the current study, the inhibition effect of CO was neglected and the reaction order with respect to CO_2 was assumed to be first order. The commonly used random pore model (RPM; see eq. 3) was applied to model the gasification behavior of the single feedstocks of SG, FC, and AFC at the respective experimental conditions.

$$\frac{dX}{dt} = k_j \cdot (1 - X) \cdot \sqrt{1 - \Psi \cdot (1 - X)} \tag{3}$$

For each temperature, 2 parameters (i.e., reaction rate constant k_j and a structural parameter Ψ) were estimated based on a non-linear least-squares method. The details for the kinetic parameter estimation and modeling techniques used are described in our previous publication[14].

4.2 Mixed Feedstock

The gasification of the mixed feed (SG/FC and SG/AFC) was modeled based on eq. 4

$$X_{mix} = \beta \cdot X'_{FF} + (1 - \beta) \cdot X'_{SG} \quad (4)$$

where X'_{FF} and X'_{SG} denote the conversions of the fossil fuel (FC, AFC) and SG in the mixture, respectively, assuming interaction between them as described above.

The gasification rate of each constituent (dX'/dt) follows the random pore model (RPM) with their corresponding kinetic parameters (see Section 4.1) with the inclusion of an additional synergism/antagonism parameter s_i that describes the deviation from the non-interacting case as illustrated in eqs. 5 and 6.

$$\frac{dX'_{SG}}{dt} = s_{SG} \cdot k_{SG} \cdot (1 - X'_{SG}) \cdot \sqrt{1 - \Psi_{SG} \cdot (1 - X'_{SG})} \quad (5)$$

$$\frac{dX'_{FF}}{dt} = s_{FF} \cdot k_{FF} \cdot (1 - X'_{FF}) \cdot \sqrt{1 - \Psi_{FF} \cdot (1 - X'_{FF})} \quad (6)$$

Here s_{SG} represents the inhibition of the switchgrass conversion rate (antagonistic parameter), while s_{FF} represents the acceleration (synergistic parameter) of the fossil fuel conversion rate. Eq. 5 is valid until complete conversion of switchgrass char (i.e., $X'_{SG} < 1$), thereafter $\frac{dX'_{SG}}{dt} = 0$ (for X'_{SG} =1), while eq. 6 is valid over the whole conversion range of the fossil fuel sample (longer time frame). Note, the term inhibition s_{SG} does not refer to catalyst inhibition, it refers to the decrease in the SG gasification rate due to potassium transfer to the non-biomass sample. Thus, the potassium does not catalyze the SG conversion.

Parameter estimation will be used to determine s_{SG} and s_{FF} using the experimental data obtained for gasification of the mixed feedstock at different temperatures (presented in section 3).

The synergism/antagonism parameter, s_i, can have values of $s_{FF} \geq 1$ presenting synergism (i.e., an increase of the reaction rate for the fossil fuel), while values of $0 < s_{SG} \leq 1$ denotes a decline in the gasification rate for SG, indicating an inhibition. The lower the value for s_{SG} the higher is the inhibition. For $s_i = 1$ (unity), eqs. 5 and 6 would be equal to the standard random pore model (eq. 6) designating neither inhibition nor acceleration.

In the present work four assumptions regarding the synergism/antagonism (i.e., acceleration/ inhibition) parameter were tested as summarized in Table 2. The parameters s_{SG} and s_{FF} had either a constant value (model 1 and A) or were a function of the SG conversion (e.g., linear, square root, non-linear) representing the effect of interparticle potassium mobility.

The numbers (1-4) describe the antagonistic (inhibition) parameter s_{SG}, while the letters (A-D) describe the behaviour of the synergistic (acceleration) parameter s_{FF}. The equations given in Table 2 include the constants, a_{SG} and a_{FF}. Possible effects these synergism/antagonism parameters on co-gasification reactions are illustrated in Figure 3 for $a_{SG} = 0.5$ and $a_{FF} = 2.0$. Since the time at which SG is completely converted in the mixed feed is not known (t'_{SG} at $X'_{SG} = 1$; $t'_{SG} > t_{SG}$), this time is determined during parameter estimation as well as the synergistic and antagonistic parameters, a_{SG} and a_{FF}, respectively. The parameters will be determined for each temperature separately, as the model describing the effect of interparticle potassium mobility might change with temperature.

4.3 Model Discrimination

16 possible combinations of the synergistic/antagonistic models exist to predict the co-gasification behaviour. The Akaike information criterion (*AIC*) was applied for model discrimination[18]. Based on the assumption of normally distributed errors, the *AIC* was calculated as follows:

$$AIC = m\frac{2}{n} + ln\left\{\frac{2}{n} \cdot RSS\right\} \tag{7}$$

where m, n and RSS are the number of estimated parameters, number of observations, and the sum of squares of residuals, respectively. The model with the lowest *AIC* value is the preferred model.

In addition, the R^2 values, which indicate the fit of the calculated values, were calculated. The software package Athena Visual Studio® v14.2 was used for kinetic parameter estimation and model discrimination[19].

5 Modeling Results and Discussion

5.1 Single Feedstock:

Based on the random pore model (*RPM*; eq. 2), the reaction rate constant k_j and structural parameter Ψ were estimated for each of the single feedstocks at each temperature. The results are summarized in Table 3. The narrow confidence interval of the estimated parameters as well as high R^2 values show that the estimated parameters present a good fit with the experimental data (Figure 4). The structural parameter increased with increasing temperature in the case of SG denoting an increasing surface area.

5.2 Mixed feedstock

The results of parameter estimation for SG/FC and SG/AFC at different temperatures are summarized in Tables 4 to 8 and depicted in Figures 5 to 7. The models have been ranked in descending order of preference based on the *AIC*.

5.2.1 Switchgrass/Fluid coke

For the SG/FC mixture at 850°C, model 3-B shows the lowest *AIC* value of -9.68, while at 950°C, 2-B would be favoured with AIC value of -9.86 (Tables 4 and 5). Tables 4 and 5 indicate that the first four models (3-B, 4-B, 1-B and 2-B) are statistically similar. Thus, it is difficult favor one over another. However, the results indicate clearly that the FC acceleration follows a linear relationship (Model B, $s_{FF} = (1 + X'_{SG} \cdot a_{FF})$]). The value for a_{FF} decreased with increasing temperature (a_{FF}

= 4.14 at 850°C and a_{FF} = 1.76 at 950°C) indicating a lower acceleration/ synergistic effect. For SG, values for a_{SG} decreased also with increasing temperature for (i.e., model 3 a_{SG} = 0.65 at 850°C to a_{SG} = 0.45 at 950°C and model 4 a_{SG} = 1.79 at 850°C to a_{SG} = 0.99 at 950°C). The decrease in the a_{FF} and a_{SG} can be explained by less potassium transfer from the SG to FC and/or to partial evaporation of potassium at 950°C (lower K/Al ratio)[5]. At higher temperature potassium might also react with alumina and silica from the switchgrass ash to form an inert potassium-aluminosilicate. The synergistic parameter, a_{FF} could not be determined for the non-linear assumption (Model D) as it always reached the upper-bound value during parameter estimation. Thus, this model will not be considered for future SG/FC feedstock co-gasification modelling.

The calculated conversions for the SG/FC mixture were in good agreement with the observed experimental values at 850°C and 950°C (Figure 5). Figure 5 also illustrates the conversion as a function of time for the switchgrass (X'_{SG}) and fluid coke (X'_{FF}) in the mixture. SG as single feed, needed approximately 1.5 h and 18 min to be completely gasified at 850°C and 950°C, respectively, while within the mixture SG is converted after 4 h and 30 min at 850°C and 950°C, respectively. Fluid coke on the other hand is converted after 10 h and 8 h at 850°C and 950°C within the mixture, respectively, which is much faster than the gasification of the single feed.

5.2.2 Switchgrass/Ash-free coal

In the case of SG/AFC mixtures, model 1-B [where, $s_{SG} = (a_{SG})$ and $s_{FF} = (1 + X_{SG} \cdot a_{FF})$] was found to be favoured at 750°C and 850°C, see Tables 6 and 7 with the lowest *AIC* value of -8.56 and -11.39, respectively. At 950°C, models 1-A, 1-B and 1-C were statistically equal. The results indicate that the inhibition parameter s_{SG} was independent of SG conversion, which was most likely a result of the interaction of the feedstocks during the pyrolysis phase as the AFC sample was directly used (not as a char). The acceleration of the gasification rate of AFC follows with the highest probability a linear relationship in the SG conversion (model B).

For a few models the parameters could not be estimated as they reached their upper or lower bound values indicate that these models were not applicable.

At 750°C SG conversion was strongly inhibited (a_{SG} = 0.053). The low availability of potassium due to slow SG conversion shows a much lower conversion of the mixture compared to the non-interacting feed. Also, the SG/AFC feed interactions during the pyrolysis phase or slow AFC volatilisation further inhibited co-gasification. But the amount of SG inhibition, and thus conversion time, decreased in the mixture with increasing temperature. The synergistic effect during co-gasification is observed despite the slow conversion of SG due to high content and good mobility of potassium. Figure 6 illustrates the observed and modeled (best fit) gasification behavior of SG, AFC and the mixtures for 850°C and 950°C.

From the parameter estimation results of both SG/FC and SG/AFC co-gasification, the synergistic behaviour follows a linear relationship and increases with increasing SG conversion. Once the SG is fully converted, all the potassium from the char is completely available for the non-biomass feedstock.

5.3 Influence of temperature on inhibition and acceleration parameter

Since the SG/FC co-gasification was studied only at two temperatures, the influence of the temperature on the synergistic/antagonistic parameters cannot be validated. However, in the case of SG/AFC mixtures, the antagonistic parameter s_{SG}, was not a function of the SG conversion and showed an exponential dependence with temperature. The product of $s_{SG} \cdot k_{SG}$ from eq. 5 can be lumped together and illustrated in the Arrhenius plot (Figure 7) to determine the change in the activation energy and the order of $\ln(k_i)$.

For the single feeds of SG and AFC the activation energies are 88 and 110 kJ mol^{-1}, respectively, and the pre-exponential factor is orders of magnitude larger for SG. Within the mixture the activation energy for SG' increased significantly (206 kJ mol^{-1}), whereas the activation energy for AFC' increased slightly (129 kJ mol^{-1}). The latter has been calculated based on a SG conversion of 50%, with $ln(s_{FF} \cdot k_{FF})$ and $s_{FF} = 1 + 0.5 \cdot a_{FF}$ from eq. 6. Once, SG is converted in the mixture the activation of AFC did not change much (132 kJ mol^{-1}, not shown). Ideally, the presence of a catalyst should lower the activation energy, but a slight increase with addition of SG during co-gasification of AFC was observed. The huge increase in the SG activation energy illustrates the strong inhibition especially at low temperatures that might be explained by the potassium mobility and/or the effect of the AFC pyrolysis step.

Brown et al.[3] published an apparent activation energy of 176 kJ mol^{-1} for switchgrass CO_2 gasification. However, this value was determined by the rate at 50% conversion and not via kinetic analysis using the random pore or any other models. In one of our previous kinetic studies an activation energy of 124 kJ mol^{-1} for ash-free coal was determined applying the random pore model[14].

6 Conclusions

This work aimed and showed how to quantify the synergism/antagonism effects that occur during co-gasification of potassium-rich switchgrass with ash-free coal and fluid coke by means of kinetic modeling including experiments, parameter estimation and model discrimination. The synergism/antagonism parameter were assumed to each follow four possible functions: a constant value, linear, square-root or non-linear trend. Based on the Akaike Information Criteria (*AIC*), the acceleration of the gasification rate of the non-biomass feedstock followed a linear function of the switchgrass conversion. The inhibition of the switchgrass conversion did not show a clear trend as it depends on the non-biomass feedstock and temperature. However, the interparticle potassium mobility during the co-gasification was evident. The presence of potassium in switchgrass which acts as a catalyst is clearly observed from the modeling, where the gasification rates for the fluid coke or ash-free coal in the mixture significantly increased for all temperatures studied.

Author information

Corresponding Author

* Email: jan.kopyscinski@mcgill.ca, Tel.: +1 514 398 4276

Notes: The authors declare no competing financial interest.

Acknowledgements

The authors thank Dr. Habibi for conducting the gasification experiments and Dr. Gupta for providing the ash-free coal samples. The authors would like to acknowledge the financial support from the Natural Sciences and Engineering Research Council of Canada (NSERC) and Carbon Management Canada.

Nomenclature

AIC	-	Akaike information criterion, eq. 7
a_{FF}	-	Synergistic constant
a_{SG}	-	Antagonistic constant
E_A	kJ mol^{-1}	activation energy
k_j	min^{-1}	rate constant
m	kg	mass
m	-	number of estimated parameters
n	-	number of observations (data points)
R	J mol^{-1} K^{-1}	universal gas constant = 8.314472
t	min or h	time
T	K or °C	temperature
s_{FF}	-	Synergistic parameter in fossil fuel conversion (acceleration)
s_{SG}	-	Antagonistic parameter in switchgrass conversion (inhibition)
X	-	char conversion

Greek symbols

β		mass fraction of non-biomass in the mixed feed
Ψ	-	Structural parameter for eq. 3

Abbreviations

AFC	ash-free coal
FC	fluid coke
RPM	random pore model
RSS	sum of squares of residuals
SG	switchgrass

References

(1) Krerkkaiwan, S.; Fushimi, C.; Tsutsumi, A.; Kuchonthara, P. *Fuel Process. Technol.* **2013**, *115*, 11–18.

(2) Sjöström, K.; Chen, G.; Yu, Q.; Brage, C.; Rosén, C. *Fuel* **1999**, *78* (10), 1189–1194.

(3) Brown, R. C.; Liu, Q.; Norton, G. *Biomass and Bioenergy* **2000**, *18* (6), 499–506.

(4) Lapuerta, M.; Hernandez, J. J.; Pazo, A.; Lopez, J. *Fuel Process. Technol.* **2008**, *89* (9), 828–837.

(5) Habibi, R.; Kopyscinski, J.; Masnadi, M. S.; Lam, J.; Grace, J. R.; Mims, C. A.; Hill, J. M. *Energy Fuels* **2013**, *27* (1), 494–500.

(6) Ding, L.; Zhang, Y.; Wang, Z.; Huang, J.; Fang, Y. *Bioresour. Technol.* **2014**, *173*, 11–20.

(7) Xu, C.; Hu, S.; Xiang, J.; Zhang, L.; Sun, L.; Shuai, C.; Chen, Q.; He, L.; Edreis, E. M. A. *Bioresour. Technol.* **2014**, *154*, 313–321.

(8) Yu, M. M.; Masnadi, M. S.; Grace, J. R.; Bi, X. T.; Lim, C. J.; Li, Y. *Bioresour. Technol.* **2014**, *175C*, 51–58.

(9) Masnadi, M. S.; Grace, J. R.; Bi, X. T.; Lim, C. J.; Ellis, N. *Appl. Energy* **2015**, *140*, 196–209.

(10) Fermoso, J.; Arias, B.; Gil, M. V; Plaza, M. G.; Pevida, C.; Pis, J. J.; Rubiera, F. *Bioresour. Technol.* **2010**, *101* (9), 3230–3235.

(11) Kopyscinski, J.; Rahman, M.; Gupta, R.; Mims, C. A.; Hill, J. M. *Fuel* **2014**, *117*, 1181–1189.

(12) Rahman, M.; Samanta, A.; Gupta, R. *Fuel Process. Technol.* **2013**, *115*, 88–98.

(13) Kopyscinski, J.; Habibi, R.; Mims, C. A.; Hill, J. M. *Energy & Fuels* **2013**, *27* (8), 4875–4883.

(14) Kopyscinski, J.; Habibi, R.; Mims, C. A.; Hill, J. M. *Energy Fuels* **2013**, *27* (8), 4875–4883.

(15) Cleveland, W. S. *J. Am. Stat. Assoc.* **1979**, *74* (368), 829–836.

(16) Moulijn, J. A.; Cerfontain, M. B.; Kapteijn, F. *Fuel* **1984**, *63* (8), 1043–1047.

(17) McKee, D. W. *Fuel* **1983**, *62* (2), 170–175.

(18) Akaike, H. *IEEE T. Autom. Contr.* **1974**, *19* (6), 716–723.

(19) Stewart, W. E.; Caracotsios, M. www.athenavisual.com 2010.

List of Tables

Table 1 Chemical analysis of the parent samples

Table 2 Assumptions of the synergistic parameter, s_{FF} and antagonistic parameter, s_{SG}

Table 3 Kinetic parameters of the random pore model for single feeds of switchgrass, fluid coke and ash-free coal at different temperatures

Table 4 Synergistic/antagonistic parameters, *AIC* and R^2 of the 16 models for SG/FC feed at 850°C

Table 5 Synergistic/antagonistic parameters, *AIC* and R^2 of the 16 models for SG/FC feed at 950°C

Table 6 Synergistic/antagonistic parameters, *AIC* and R^2 of the 16 models for SG/AFC feed at 750°C

Table 7 Synergistic/antagonistic parameters, *AIC* and R^2 of the 16 models for SG/AFC feed at 850°C

Table 8 Synergistic/antagonistic parameters, *AIC* and R^2 of the 16 models for SG/AFC feed at 950°C

List of Figures

Figure 1 Char conversion during CO_2 gasification of switchgrass (SG), fluid coke (FC), ash-free coal (AFC), mixture of SG/FC and SG/AFC at a) 850°C and b) 950°C. Dotted lines indicate observed and solid lines indicate non-interacting char conversion.

Figure 2 Simplified scheme of the potassium catalyzed CO_2 gasification mechanism (oxygen transfer cycle) including intra- and interparticle potassium transfer.

Figure 3 Synergistic/antagonistic behaviour of the different assumed models for $a_{SG} = 0.5$ and $a_{FF} = 2.0$, where Model 1-A: $s_i = a_i$; Model 2-B: $s_i = 1 \pm X'_{SG} \cdot a_i$; Model 3-C: $s_i = 1 \pm \sqrt{X'_{SG}} \cdot a_i$; Model 4-D: $s_i = 1 \pm \frac{X'_{SG} \cdot a_i}{(1+X'_{SG} \cdot a_i)}$

Figure 4 Observed and modeled char conversion during CO_2 gasification for a) switchgrass (SG), b) ash-free coal (AFC) and c) fluid coke (FC). Symbols represent observed data and lines the modeled values for the random pore model.

Figure 5 Observed and calculated char conversion for switchgrass and fluid coke co-gasification at a) 850°C and b) 950°C. The dotted lines represent observed values, dashed line represent non-interacting values and solid lines indicate the best fit model (3-B).

Figure 6 Observed and calculated char conversion for switchgrass and ash-free coal co-gasification at a) 850°C and b) 950°C. The dotted lines represent observed values, dashed line represent non-interacting values and solid lines indicate the best fit model (1-B).

Figure 7 Arrhenius plot for the CO_2 gasification of switchgrass (SG), ash-free coal (AFC) as single feed and in the mixture (SG' and AFC').

Table 1 Chemical analysis of the parent samples

	SG	**FC**	**AFC**
Proximate analysis (wt%), db[a]			
Volatile	76.9	6.9	69.5
Fixed carbon	16.8	91.1	30.5
Ash	6.3	2.0	~700 mg/kg [c]
Ultimate analysis (wt%), daf [a]			
Carbon, C	47.9	83.7	73.1
Hydrogen, H	6.2	1.9	4.3
Nitrogen, N	0.8	2.2	1.0
Sulfur, S	0.1	7.5	0.4
Oxygen, O[b]	45.0	4.8	21.2
Ash analysis (wt%)			
SiO_2	52.5	34.7	-
Al_2O_3	2.1	24.9	-
TiO_2	0.02	4.0	-
Fe_2O_3	0.3	10.0	-
CaO	6.4	5.4	-
MgO	6.5	2.3	-
Na_2O	1.6	2.2	-
K_2O	20.3	1.5	-
P_2O_5	5.0	0.6	-
SO_3	2.6	2.0	-

[a] db = dry basis, daf = dry and ash free, [b] calculated by difference,
[c] determined by ICP-MS (mg_{ash}/kg_{AFC}),

416 Table 2 Tested assumptions of the synergistic parameter, s_{FF} and antagonistic parameter, s_{SG}

Model	s_{SG}	Model	s_{FF}
1	a_{SG}	A	a_{FF}
2	$1 - X'_{SG} \cdot a_{SG}$	B	$1 + X'_{SG} \cdot a_{FF}$
3	$1 - \sqrt{X'_{SG}} \cdot a_{SG}$	C	$1 + \sqrt{X'_{SG}} \cdot a_{FF}$
4	$1 - \frac{X'_{SG} \cdot a_{SG}}{(1 + X'_{SG} \cdot a_{SG})}$	D	$1 + \frac{X'_{SG} \cdot a_{FF}}{(1 + X'_{SG} \cdot a_{FF})}$

417

418

419 Table 3 Kinetic parameters of the random pore model for single feeds of SG, FC and AFC at different

420 temperatures

T (°C)	***k_j (min^{-1})***		***Ψ***		***R^2***
Switchgrass (SG)					
750	$1.278 \cdot 10^{-2}$	$\pm 1.3 \cdot 10^{-4}$	0.03	± 0.02	0.998
850	$2.619 \cdot 10^{-2}$	$\pm 2.0 \cdot 10^{-4}$	1.43	± 0.05	0.999
950	$7.001 \cdot 10^{-2}$	$\pm 8.7 \cdot 10^{-4}$	8.15	± 0.30	0.999
Fluid coke (FC)					
850	$2.882 \cdot 10^{-4}$	$\pm 2.1 \cdot 10^{-6}$	15.8	± 0.30	0.999
950	$2.719 \cdot 10^{-3}$	$\pm 5.0 \cdot 10^{-6}$	0.09	± 0.01	0.999
Ash-free coal (AFC)					
750	$2.071 \cdot 10^{-4}$	$\pm 4.2 \cdot 10^{-7}$	1.39	± 0.02	0.999
850	$5.391 \cdot 10^{-4}$	$\pm 3.6 \cdot 10^{-6}$	0.75	± 0.03	0.998
950	$1.736 \cdot 10^{-3}$	$\pm 1.5 \cdot 10^{-5}$	3.05	± 0.10	0.999

421

Table 4 Synergistic/antagonistic parameters, *AIC* and R^2 of the 16 models for SG/FC feed at 850°C

Model	a_{SG}		a_{FF}		***AIC***	R^2	**Rank**
3-B	0.65	± 0.01	4.14	± 0.02	**-9.68**	0.998	**1**
4-B	1.79	± 0.04	4.12	± 0.02	-9.36	0.998	**2**
3-C	0.70	± 0.01	3.90	± 0.02	-9.33	0.998	**3**
1-B	0.58	± 0.01	4.05	± 0.02	-9.25	0.998	**4**
4-C	2.08	± 0.05	3.88	± 0.02	-9.13	0.998	**5**
3-A	0.80	± 0.01	4.60	± 0.02	-9.11	0.998	**6**
2-B	0.83	± 0.01	4.27	± 0.04	-8.86	0.997	**7**
2-C	0.91	± 0.02	4.19	± 0.07	-8.86	0.997	**7**
4-A	2.67	± 0.07	4.53	± 0.02	-8.77	0.997	**9**
1-C	0.56	± 0.01	3.81	± 0.03	-8.64	0.997	**10**
2-A	0.99	± 0.03	4.94	± 0.12	-8.53	0.996	**11**
1-A	0.51	± 0.01	4.41	± 0.03	-7.92	0.993	**12**
1-D	0.64	± 0.10	#		-3.73	0.559	**13**
2-D	0.60	± 0.22	#		-3.72	0.553	**14**
3-D	0.51	± 0.16	#		-3.72	0.556	**15**
4-D	1.10	± 0.59	#		-3.72	0.555	**16**

Upper bound value reached

Table 5 Synergistic/antagonistic parameters, *AIC* and R^2 of the 16 models for SG/FC feed at 950°C

Model	a_{SG}	a_{FF}	*AIC*	R^2	Rank
2-B	0.63 ± 0.02	1.76 ± 0.01	**-9.86**	0.998	**1**
4-B	0.99 ± 0.06	1.76 ± 0.01	**-9.80**	0.998	**2**
3-B	0.45 ± 0.02	1.76 ± 0.01	**-9.73**	0.998	**3**
2-C	0.68 ± 0.01	1.73 ± 0.01	-9.59	0.998	**4**
4-C	1.10 ± 0.08	1.72 ± 0.02	-9.48	0.997	**5**
1-B	0.76 ± 0.01	1.75 ± 0.02	-9.44	0.997	**6**
3-C	0.48 ± 0.02	1.72 ± 0.02	-9.43	0.997	**7**
2-A	0.79 ± 0.03	2.66 ± 0.02	-9.22	0.997	**8**
1-C	0.74 ± 0.02	1.72 ± 0.02	-9.17	0.997	**9**
4-A	1.34 ± 0.11	2.65 ± 0.02	-9.04	0.996	**9**
3-A	0.54 ± 0.03	2.65 ± 0.02	-8.98	0.996	**11**
1-A	0.71 ± 0.02	2.65 ± 0.02	-8.75	0.995	**12**
2-D	0.60 ± 0.17	#	-6.16	0.930	**13**
1-D	0.76 ± 0.08	#	-6.15	0.930	**14**
4-D	0.93 ± 0.41	#	-6.15	0.929	**15**
3-D	0.43 ± 0.13	#	-6.12	0.928	**16**

Upper bound value reached

Table 6 Synergistic/antagonistic parameters, *AIC* and R^2 of the 16 models for SG/AFC feed at 750°C

Model	a_{SG}	a_{FF}	*AIC*	R^2	**Rank**
1-B	0.05 ± 0.00	4.49 ± 0.20	**-8.56**	0.997	**1**
1-C	0.05 ± 0.00	3.34 ± 0.34	-7.69	0.993	**2**
1-A	0.05 ± 0.01	2.73 ± 0.66	-6.64	0.980	**3**
1-D	0.08 ± 0.00	#	-6.22	0.970	**4**
2-A	0.93 ± 0.07	ǂ	-3.42	0.508	**5**
3-A	0.63 ± 0.05	1.21 ± 0.08	-3.29	0.440	**6**

Upper bound value reached, ǂ Lower bound value reached

Table 7 Synergistic/antagonistic parameters, *AIC* and R^2 of the 16 models for SG/AFC feed at 850°C

Model	a_{SG}	a_{FF}	*AIC*	R^2	**Rank**
1-B	0.21 ± 0.00	9.10 ± 0.04	**-11.39**	0.999	**1**
1-C	0.17 ± 0.00	9.50 ± 0.09	**-11.22**	0.999	**2**
1-A	0.14 ± 0.02	7.91 ± 1.24	-7.65	0.995	**3**
3-B	#	5.96 ± 0.19	-5.60	0.959	**4**
3-C	#	5.14 ± 0.18	-5.35	0.947	**5**
3-A	#	5.19 ± 0.16	-5.05	0.929	**6**
2-B	#	5.06 ± 0.24	-4.79	0.908	**7**
2-C	#	4.55 ± 0.22	-4.66	0.895	**8**
2-A	#	4.92 ± 0.20	-4.49	0.875	**9**
4-B	#	4.33 ± 0.26	-4.25	0.841	**10**
4-C	#	4.02 ± 0.25	-4.17	0.827	**11**
4-A	#	4.60 ± 0.24	-4.05	0.807	**12**
1-D	0.32 ± 0.04	#	-3.39	0.626	**13**
3-D	0.93 ± 0.07	#	-3.34	0.606	**14**

Upper bound value reached

Table 8 Synergistic/antagonistic parameters, *AIC* and R^2 of the 16 models for SG/AFC feed at 950°C

Model	a_{SG}	a_{FF}	***AIC***	R^2	**Rank**
1-A	0.42 ± 0.00	6.89 ± 0.03	**-9.17**	0.998	**1**
1-C	0.49 ± 0.00	6.73 ± 0.04	**-9.17**	0.998	**1**
1-B	0.53 ± 0.00	7.21 ± 0.05	**-9.09**	0.998	**3**
3-C	0.79 ± 0.01	6.91 ± 0.07	-8.54	0.997	**4**
3-B	0.74 ± 0.01	7.35 ± 0.08	-8.47	0.997	**5**
3-A	0.87 ± 0.01	7.23 ± 0.08	-8.22	0.996	**6**
2-C	#	7.79 ± 0.10	-7.54	0.991	**7**
2-B	0.88 ± 0.02	7.41 ± 0.17	-7.45	0.991	**8**
2-A	#	7.53 ± 0.10	-6.99	0.985	**9**
4-B	#	6.56 ± 0.12	-6.84	0.983	**10**
4-C	#	6.13 ± 0.12	-6.58	0.978	**11**
4-A	#	6.47 ± 0.13	-6.18	0.966	**12**
1-D	0.63 ± 0.13	#	-3.03	0.226	**13**
2-D	0.63 ± 0.33	#	-3.03	0.221	**14**
3-D	0.52 ± 0.24	#	-3.03	0.224	**15**

Upper bound value reached

437 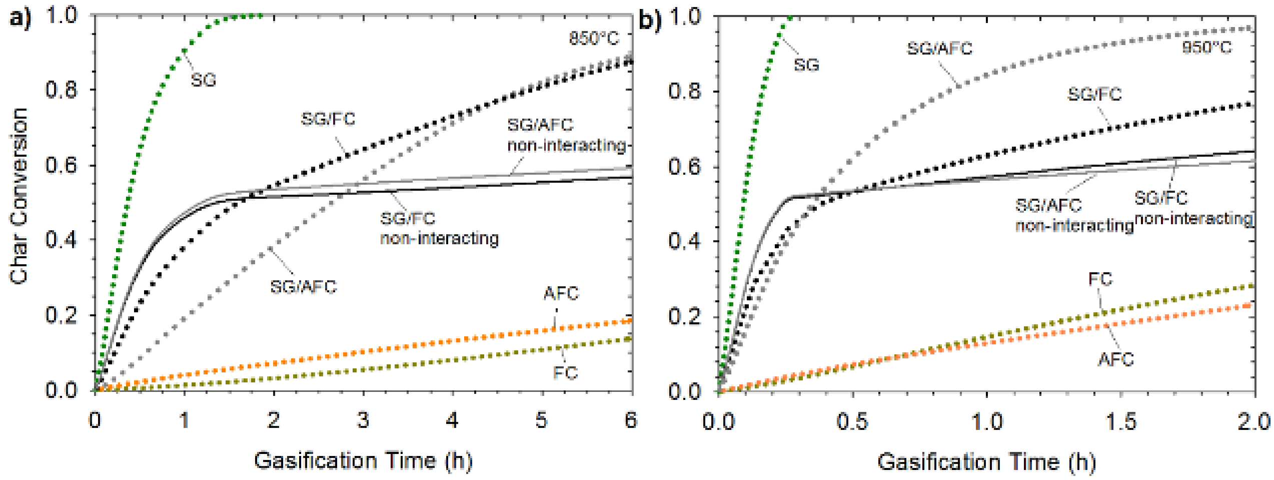

438 Figure 1 Char conversion during CO_2 gasification of switchgrass (SG), fluid coke (FC), ash-free coal

439 (AFC), mixture of SG/FC and SG/AFC at a) 850°C and b) 950°C. Dotted lines indicate observed and solid

440 lines indicate non-interacting conversion.

441

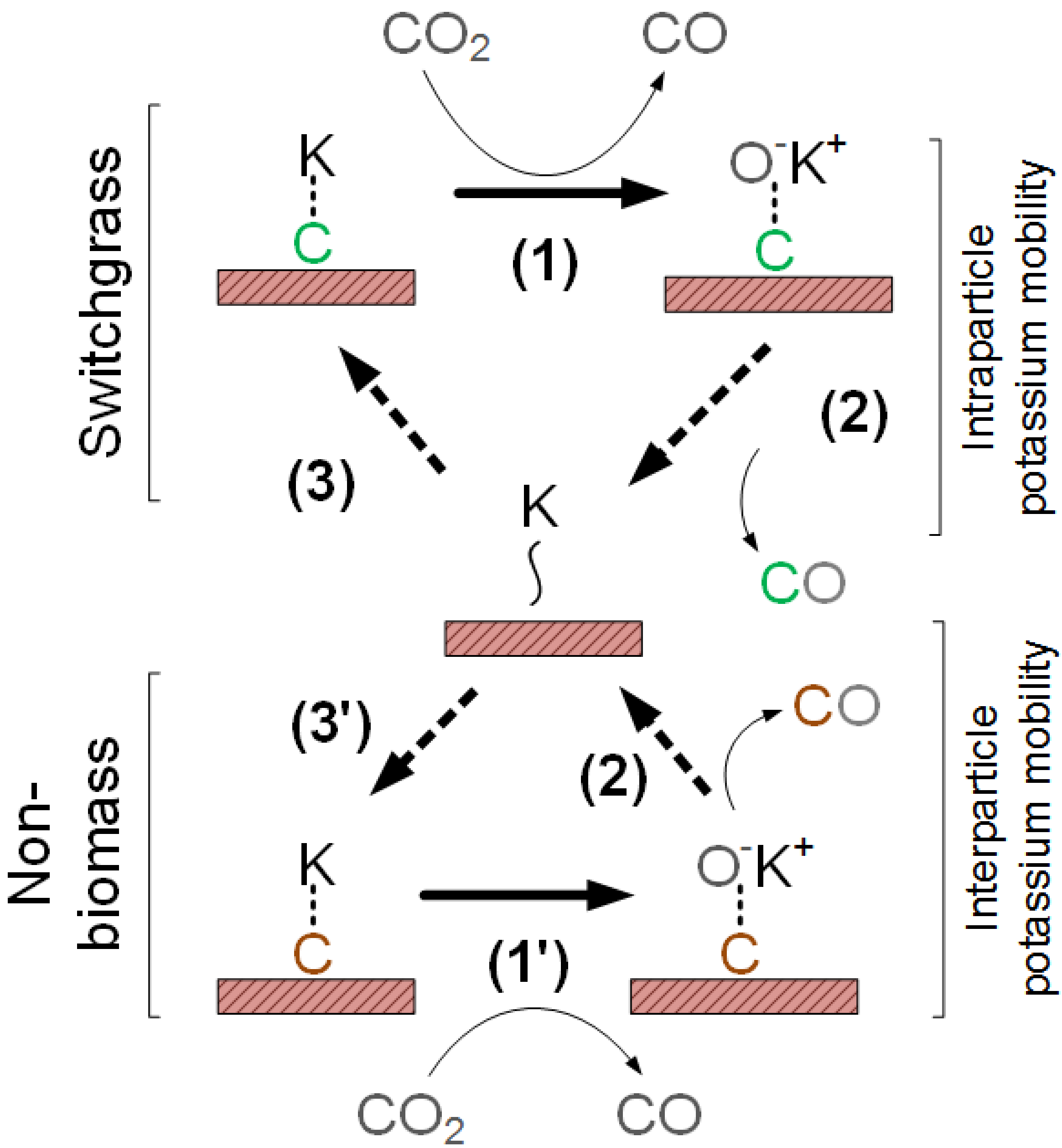

Figure 2 Simplified scheme of the potassium catalyzed CO2 gasification mechanism (oxygen transfer cycle) including intra- and interparticle potassium transfer.

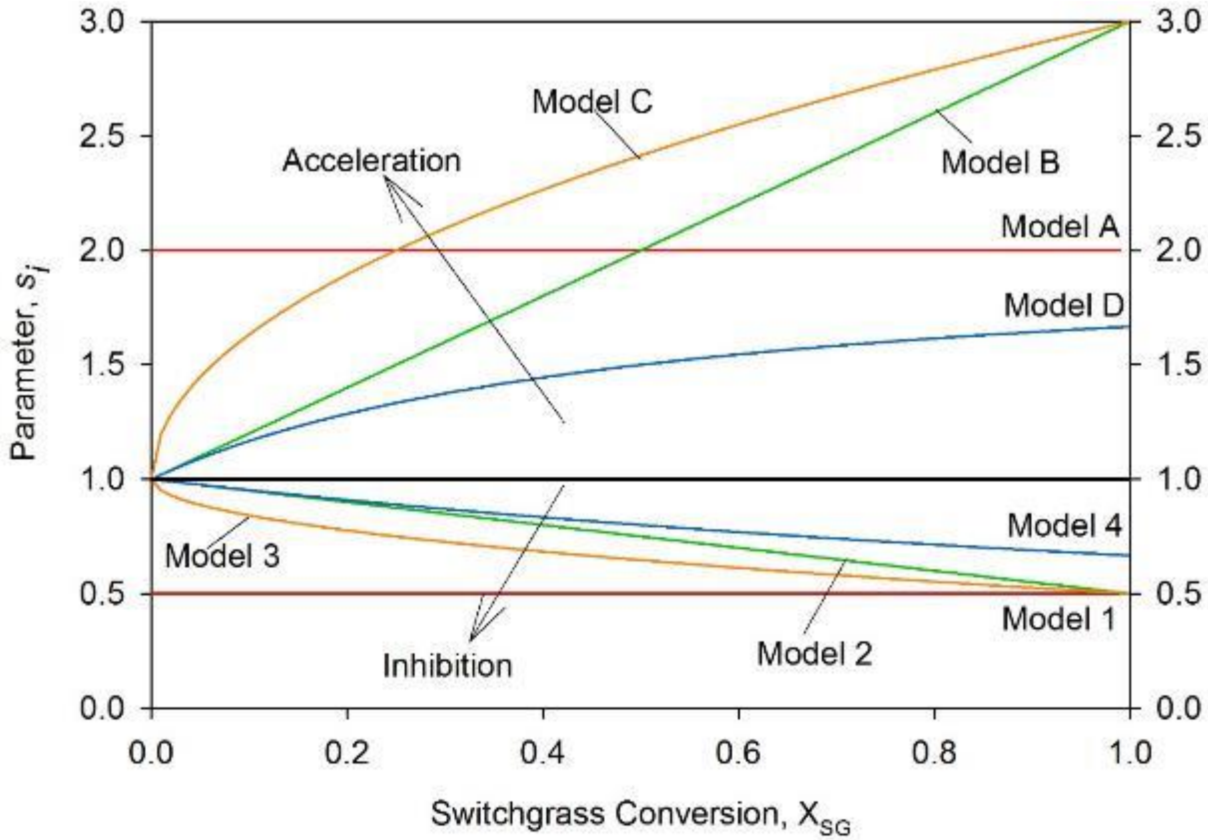

448 Figure 3 Synergistic/antagonistic behaviour of the different assumed models for a_{SG} = 0.5 and a_{FF} = 2.0, where Model 1-A: $s_i = a_i$; Model 2-B: $s_i = (1 \pm X'_{SG} \cdot a_i)$; Model 3-C: $s_i = \left(1 \pm a_i \cdot \sqrt{X'_{SG}}\right)$; Model 4-D: $s_i = \left(1 \pm \frac{X'_{SG} \cdot a_i}{1 + X'_{SG} \cdot a_i}\right)$

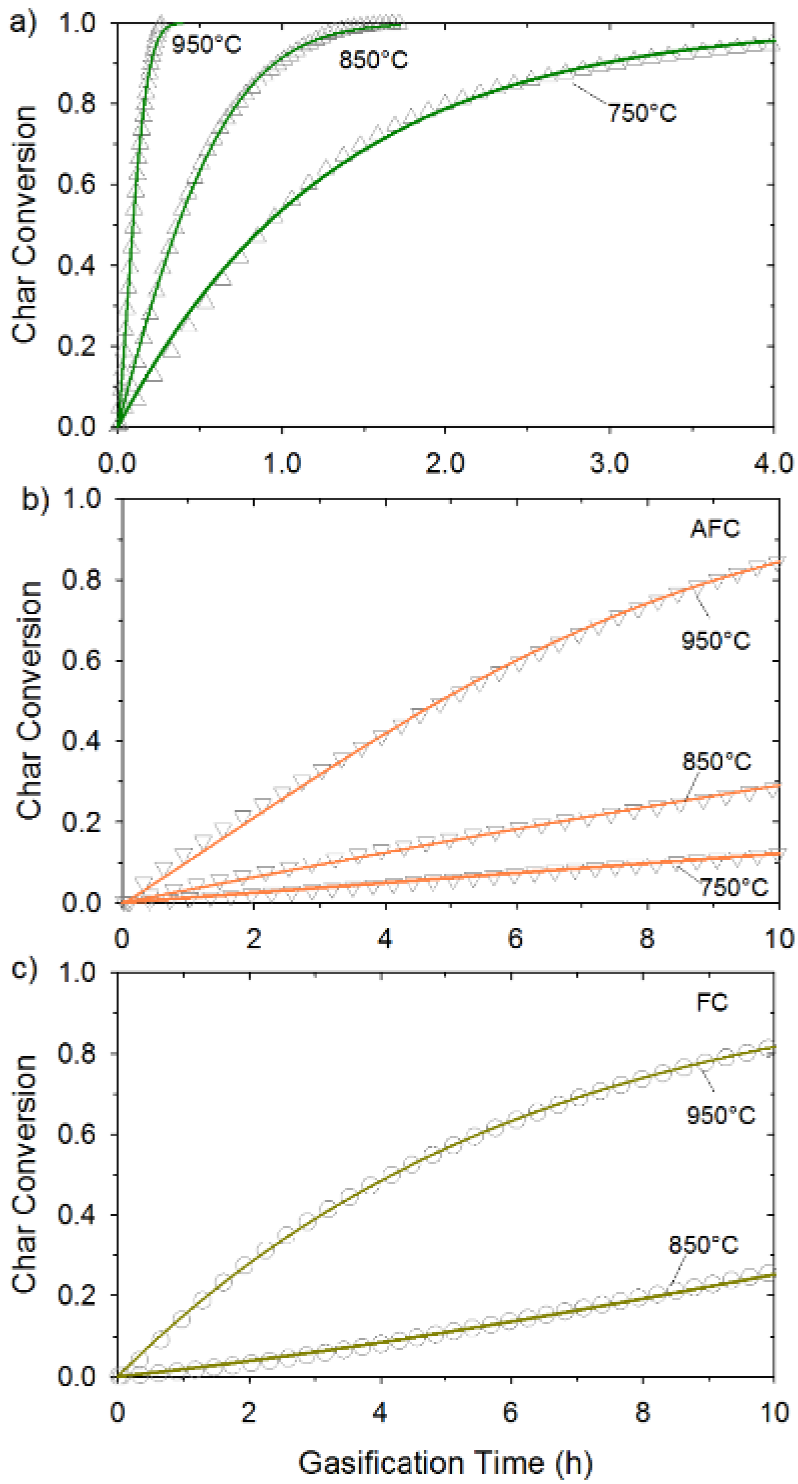

Figure 4 Observed and modeled char conversion during CO_2 gasification for a) switchgrass (SG), b) ash-free coal (AFC) and c) fluid coke (FC). Symbols represent observed data and lines the modeled values for the random pore model.

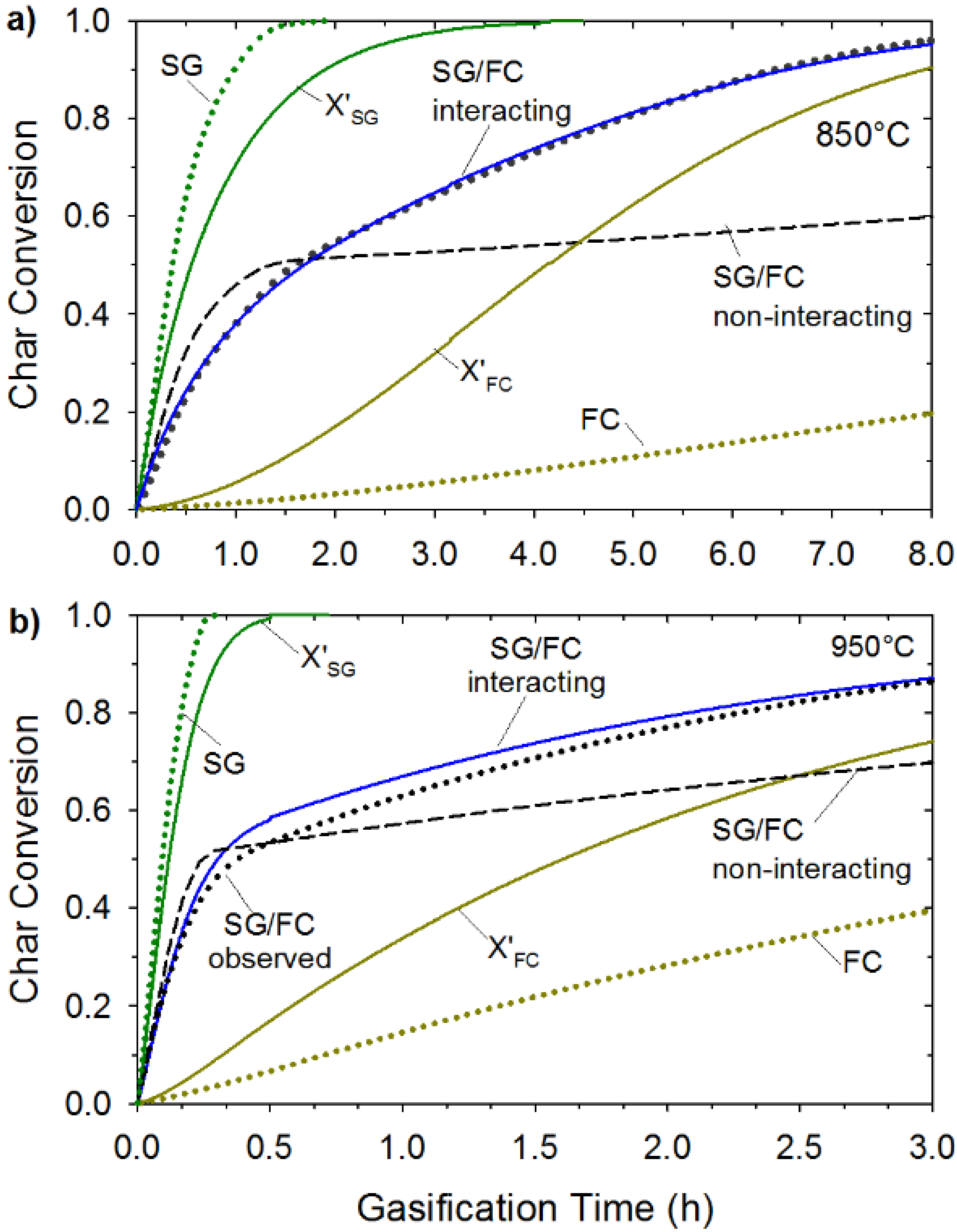

Figure 5 Observed and calculated char conversion for switchgrass and fluid coke co-gasification at a) 850°C and b) 950°C. The dotted lines represent observed values, dashed line represents non-interacting values and solid lines indicate the best-fit model (3-B).

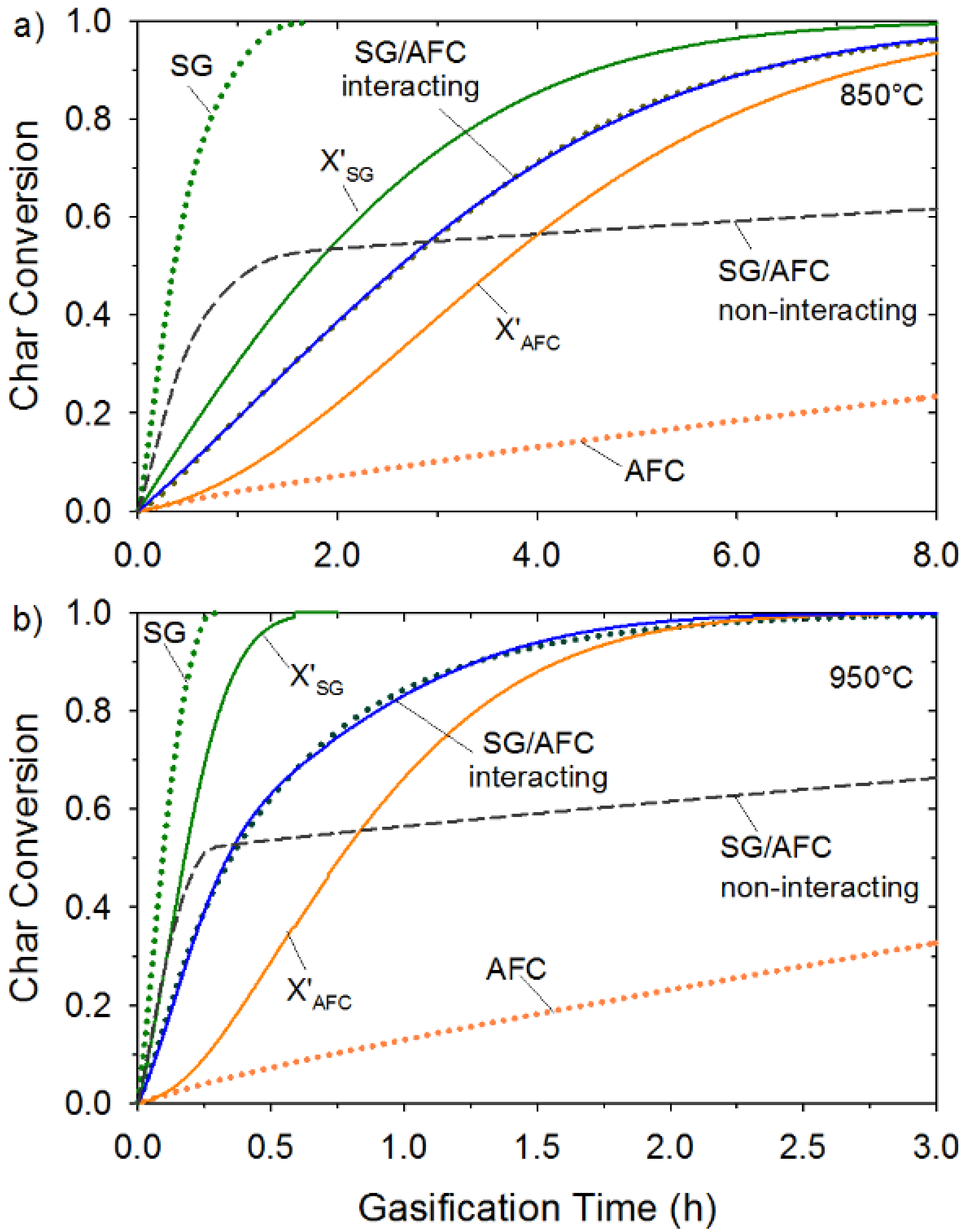

Figure 6 Observed and calculated char conversion for switchgrass and ash-free coal co-gasification at a) 850°C and b) 950°C. The dotted lines represent observed values, dashed lines represent non-interacting values and solid lines indicate the best-fit model (1-B).

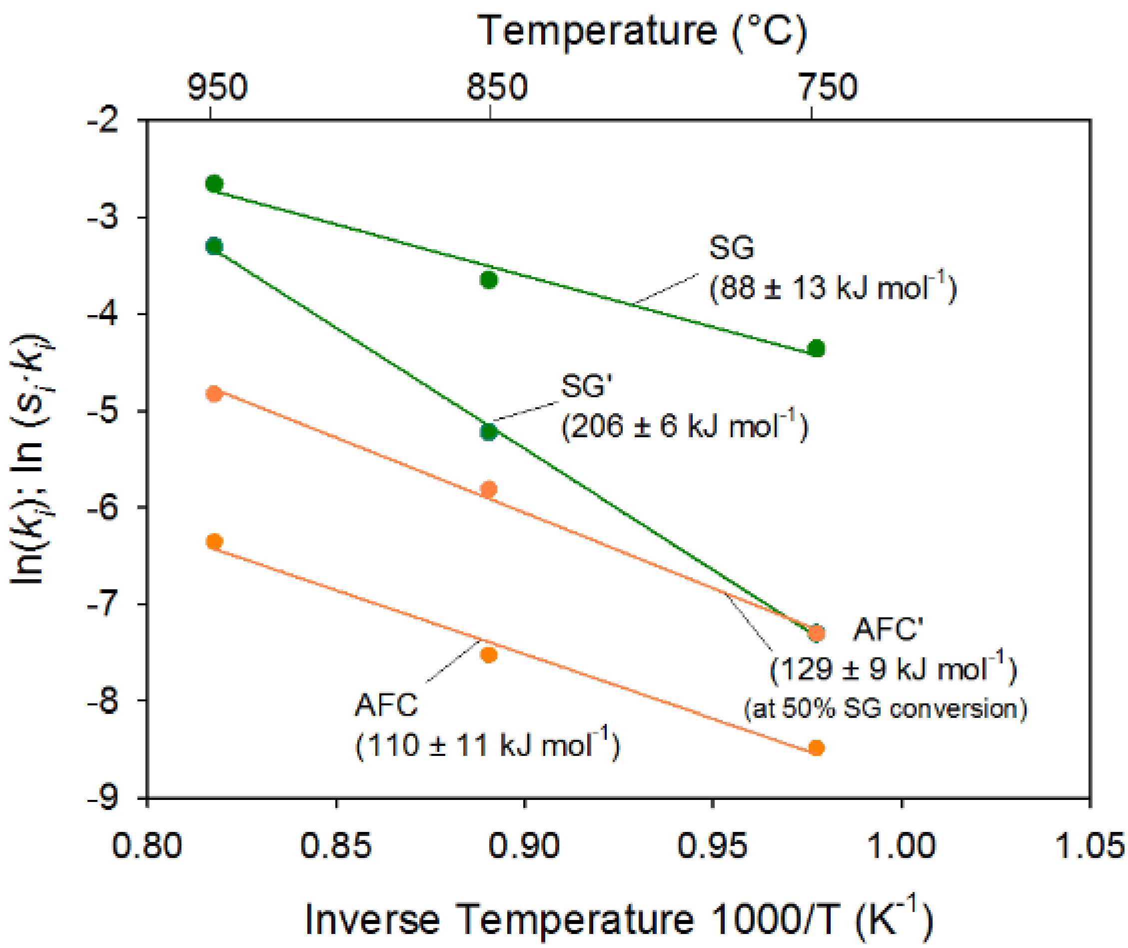

Figure 7 Arrhenius plot for the CO_2 gasification of switchgrass (SG) and ash-free coal (AFC) as single feeds or within a mixture (SG' and AFC')